ChemPubSoc Europe
DOI: 10.1002/chem.201303801
CHEMISTRY
A European Journal
Full Paper

Metal–Organic Frameworks

Enhancing CO_2 Separation Ability of a Metal–Organic Framework by Post-Synthetic Ligand Exchange with Flexible Aliphatic Carboxylates

Dae Ho Hong and Myunghyun Paik Suh*[a]

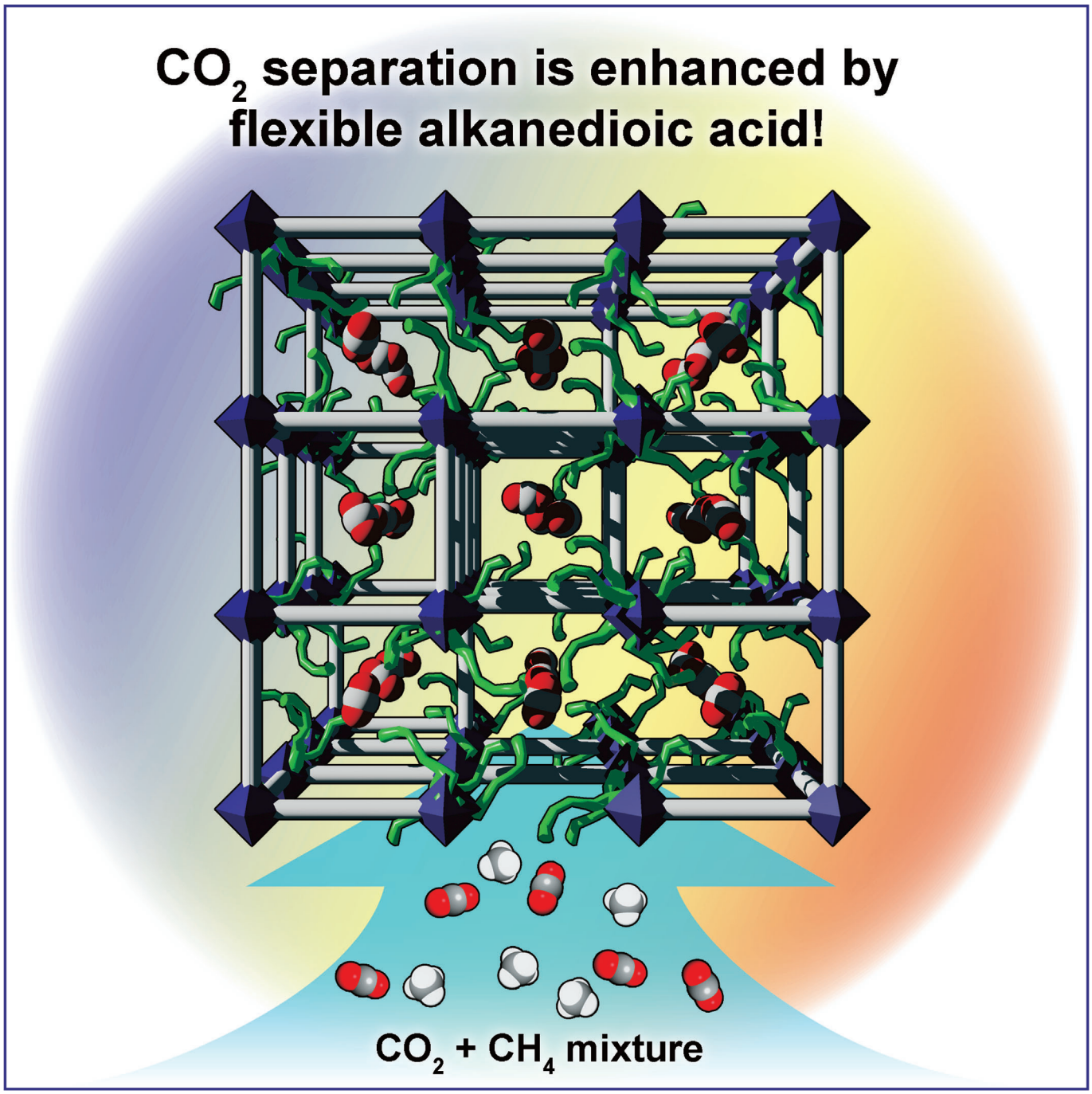

Abstract: A series of porous metal–organic frameworks having flexible carboxylic acid pendants in their pores (UiO-66-AD*n*: $n=4$, 6, 8, and 10, where *n* denotes the number of carbons in a pendant) has been synthesized by post-synthetic ligand exchange of terephthalate in UiO-66 with a series of alkanedioic acids ($HO_2C(CH_2)_{n-2}CO_2H$). NMR, IR, PXRD, TEM, and mass spectral data have suggested that a terephthalate linker in UiO-66 was substituted by two alkanedioate moieties, resulting in free carboxyl pendants in the pores. When post-synthetically modified UiO-66 was partially digested by adjusting the amount of added HF/sample, NMR spectra indicated that the ratio of alkanedioic acid/terephthalic acid was increased with smaller amounts of acid, implying that the ligand substitution proceeded from the outer layer of the particles. Gas sorption studies indicated that the surface areas and the pore volumes of all UiO-66-AD*n*s were decreased compared to those of UiO-66, and that the CO_2 adsorption capacities of UiO-66-AD*n* ($n=4$, 8) were similar to that of UiO-66. In the case of UiO-66-AD6, the CO_2 uptake capacity was 34% higher at 298 K and 58% higher at 323 K compared to those of UiO-66. It was elucidated by thermodynamic calculations that the introduction of flexible carboxyl pendants of appropriate length has two effects: 1) it increases the interaction enthalpy between the host framework and CO_2 molecules, and 2) it mitigates the entropy loss upon CO_2 adsorption due to the formation of multiple configurations for the interactions between carboxyl groups and CO_2 molecules. The ideal adsorption solution theory (IAST) selectivity for CO_2 adsorption over that of CH_4 was enhanced for all of the UiO-66-AD*n*s compared to that of UiO-66 at 298 K. In particular, UiO-66-AD6 showed the most strongly enhanced CO_2 uptake capacity and significantly increased selectivity for CO_2 adsorption over that of CH_4 at ambient temperature, suggesting that it is a promising material for sequestering CO_2 from landfill gas.

Introduction

Metal–organic frameworks have been considered as promising materials for separating CO_2 from landfill gas and industrial flue gas due to their high surface areas and the chemical tunability of their pores.[1,2] However, MOFs commonly show poor stability toward moisture, and when hydrated their gas-uptake capacities are severely reduced.[3] Therefore, water-stable MOFs such as ZIFs,[4] MIL-101,[5] and UiO-66[6] have attracted great attention and have been employed for post-synthetic modifications (PSMs),[7–9] in which some or all of the building blocks in a synthesized MOF are changed. PSMs provide alternative routes for functionalizing MOFs, and thus enable the creation of MOFs that cannot be obtained by normal solvothermal synthesis. Such methods have been demonstrated to be effective in the introduction of functional groups,[10] the insertion, removal, or exchange of organic linkers,[7,8,11,12] as well as the exchange of framework metal ions.[9,13]

To apply MOFs as carbon dioxide capture materials, they should have high CO_2 adsorption capacities and high selectivities for CO_2 adsorption over that of other gases such as CH_4 or N_2. A high isosteric heat value for CO_2 adsorption generally leads to a high uptake capacity and increased selectivity for CO_2 adsorption over that of other gases, but a higher energy may be required for regeneration of the adsorbent.[1] Many studies have been performed with the aim of increasing the isosteric heats of CO_2 adsorption in MOFs. It is important to note that the isosteric heat is a differential enthalpy of adsorption, which does not include the entropic effect. To fully understand the adsorption phenomenon, free energy (*G*) or chemical potential (μ) should be taken into consideration. One of the useful thermodynamic tools for analyzing an adsorption isotherm is consideration of the desorption functions (*G*, *H*, *S*) suggested by Myers.[14] These functions provide a complete thermodynamic description for an adsorption system with positive quantities, and the desorption free energy is the minimum isothermal energy required for regeneration of the adsorbent.

It has been reported that the introduction of flexible pendants bearing hydroxyl, amine, or ether functional groups into MOFs increases the selectivity for CO_2 adsorption over that of other gases, since closely located flexible pendants interlock with each other to act as a gate[15] or provide polar adsorption sites for CO_2 molecules.[10,16,17] To the best of our knowledge, the entropic effect of a flexible pendant incorporated into an MOF for CO_2 separation has not hitherto been explored. However, the entropy value must be considered in order to make a comprehensive assessment of the effect of a flexible pendant on CO_2 adsorption. It has been reported that separation of alkane isomers by a zeolite material is driven by differences in the degree of reduction of the rotational entropy of each alkane in the pores.[18] Since the adsorption process is governed by the change in the free energy ($\Delta G=\Delta H-T\Delta S$) and the contribution of the entropy to the free energy increases with increasing temperature, a reduction of the entropy loss associated with gas adsorption must be advantageous for obtaining improved gas uptake at high temperatures. This view inspired us to introduce flexible alkyl pendants into an MOF and to investigate their entropy effect on the adsorption of CO_2.

Herein, we report post-synthetic ligand exchange of UiO-66, a water-stable MOF, with various flexible alkanedioic acids ($HO_2C(CH_2)_{n-2}CO_2H$), which afforded a series of modified UiO-

[a] *D. H. Hong, Prof. M. P. Suh*
Department of Chemistry, Seoul National University
Seoul 151-747 (South Korea)
Fax: (+82) 2-886-8516
E-mail: mpsuh@snu.ac.kr

Supporting information for this article is available on the WWW under http://dx.doi.org/10.1002/chem.201303801.

66-AD*n* ($n=4$, 6, 8, and 10). During the post-synthetic ligand exchange, a single terephthalate ligand was substituted by two flexible alkanedioate ligands. This unique 1:2 ligand substitution has not previously been achieved by post-synthetic modification of MOFs.[7,8,12] For various alkanedioic acids, the degree of ligand substitution increased as the length of the acid increased. By partial digestion of the solid samples, it has also been revealed for the first time that post-synthetic ligand substitution proceeds from the outer layer of the solid instead of homogeneously in the whole crystal. Interestingly, gas adsorption studies showed that UiO-66-AD6 led to a smaller decrease in CO_2 uptake at elevated temperatures than did UiO-66. According to thermodynamic calculations based on Myers' desorption functions, the high CO_2 uptake capacities of UiO-66-AD6 at 298 K and 323 K are related to an increase in the free energy loss upon CO_2 adsorption, which is caused by the mitigated entropy loss. This entropy effect suggests that an appropriately adjusted length of flexible pendant would allow for various interaction modes between carboxyl groups and CO_2 molecules. The introduction of carboxyl pendants increased the low-coverage isosteric heats of CO_2 adsorption in all of the UiO-66-AD*n*s compared to UiO-66, with the maximum effect being observed for UiO-66-AD6. IAST selectivities for CO_2 adsorption over CH_4 adsorption increased for all of the UiO-66-AD*n*s due to stronger interactions between the carboxylic acid groups and CO_2 molecules.[19] In particular, UiO-66-AD6 proved to be the most promising for CO_2 sequestration from landfill gas at ambient temperature, since it showed the highest uptake capacity and significantly increased selectivity for CO_2 adsorption over that of CH_4.

Results and Discussion

Post-synthetic modification of UiO-66

UiO-66 was prepared by heating a solution of $ZrCl_4$ and terephthalic acid (H_2BDC) in DMF at 120 °C for 24 h, according to the previously reported method.[6] The framework of UiO-66 consists of a very stable $Zr_6O_4(OH)_4(CO_2)_{12}$ cluster extending in twelve directions to form a cubic closed packed (ccp) structure, which generates tetrahedral and octahedral cages of sizes 8 Å and 11 Å, respectively. These cages are connected by a triangular window of size 6 Å (Figure S1 in the Supporting Information).[6]

For the post-synthetic ligand exchange of UiO-66, its guest solvent molecules were removed by the heat-evacuation method at 100 °C. The desolvated sample was then immersed in an aqueous solution of the requisite alkanedioic acid (0.067 M) at 60 °C for five days, adjusting the pH to 7 with KOH and HCl (see the Experimental Section).[6,8] As new incoming ligands, succinic acid ($n=4$), adipic acid ($n=6$), suberic acid ($n=8$), and sebacic acid ($n=10$) were employed. It should be noted here that adipic acid ($n=6$) is similar in length to the terephthalate linker of UiO-66 (see Table S1 in the Supporting Information). To remove any alkanedioic acid residing in the pores, the resulting samples were immersed in MeOH and the supernatant was replenished with fresh MeOH every 12 h for two days. After activating the samples by heat treatment at 100 °C for 12 h, the dried samples, UiO-66-AD*n*s, were obtained.

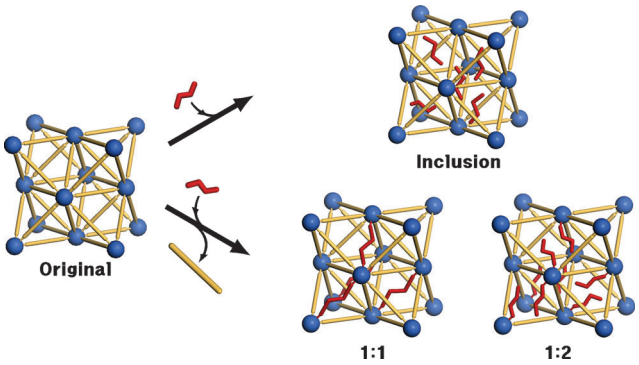

Figure 1. Three possible ways of introducing new flexible functional pendants into UiO-66. The 1:1 model represents a situation whereby an alkanedioate ligand replaces a terephthalate ligand, whereas in the 1:2 model two alkanedioate ligands substitute terephthalate leaving uncoordinated carboxylic acid groups. In the inclusion model, ligand substitution does not occur. Color scheme: metal cluster, blue; terephthalate, orange; alkanedioate, red.

For the introduction of new flexible linkers in UiO-66, three distinct modes are possible (Figure 1): 1) 1:1 substitution of a terephthalate ligand with an alkanedioate ligand of similar length; 2) 1:2 substitution of a terephthalate ligand with two alkanedioate ligands, which leaves free carboxyl pendants in the structure; and 3) simple inclusion of the alkanedioic acid in the pores of the framework, without substitution. Various experimental results suggest that each terephthalate ligand in UiO-66 is substituted by two flexible alkanedioate ligands. ^{1}H NMR spectra of samples digested in [D$_6$]DMSO containing HF revealed that the alkanedioate contents of the resulting solutions were 15.9% for UiO-66-AD4, 17.3% for UiO-66-AD6, 23.2% for UiO-66-AD8, and 49.6% for UiO-66-AD10 (Figure 2 and Table S2). In an additional experiment, UiO-66 was immersed in a mixture of succinic acid, adipic acid, and suberic acid at the same concentrations. Subsequent activation gave a product that contained 3% succinate, 5% adipate, and 15% suberate (Figure S2). The greater incorporation of longer alkanedioate ligands may be attributed to the stronger van der Waals interaction between the longer alkane chains in UiO-66-AD*n*. The fact that all of the alkanedioate ligands could be incorporated into UiO-66 irrespective of their lengths, without changing the periodic structure, as evidenced by PXRD patterns (Figure 3), coupled with the observation of free carboxylic acid peaks in the region $\tilde{\nu}=1703$–1718 cm^{-1} in the IR spectra of UiO-66-AD*n*s (Figure S3), strongly disfavored the 1:1 substitution model. In the case of UiO-66-AD6, however, a 1:1 substitution mode may be mixed with another substitution mode since the length of an adipic acid ligand is almost identical to that of terephthalate. It has been reported that an organic ligand in an MOF can be substituted in a 1:1 fashion by another ligand of identical length.[7,8] The following data exclude the possibility that alkanedioic acids are simply included in the pores. 1) A peak attributable to a hydrated terephthalate ion ($HBDC{\cdot}H_2O^-$) was found in the mass spectrum ($m/z=183$) of

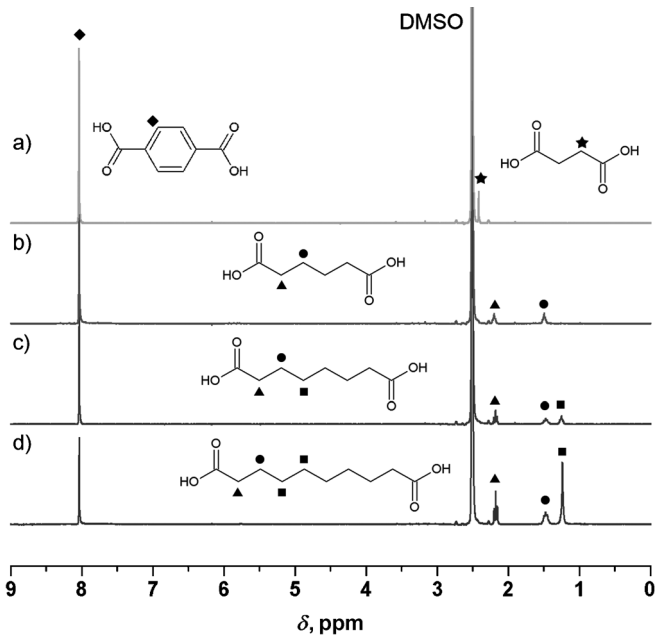

Figure 2. ^{1}H NMR spectra of UiO-66-AD*n*s after digestion with hydrofluoric acid in [D_6]DMSO solution: a) UiO-66-AD4, b) UiO-66-AD6, c) UiO-66-AD8, and d) UiO-66-AD10. Water peaks have been suppressed for clarity.

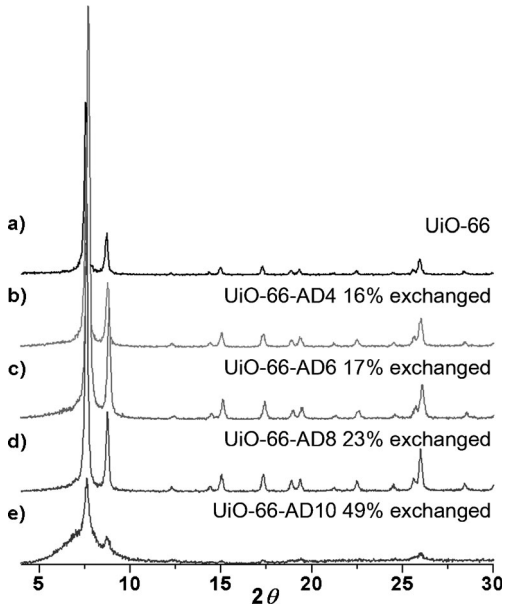

Figure 3. Powder X-ray diffraction patterns for UiO-66-AD*n*s activated by the heat-evacuation method at 100 °C: a) UiO-66, b) UiO-66-AD4, c) UiO-66-AD6, d) UiO-66-AD8, and e) UiO-66-AD10.

an adipic acid solution in which UiO-66 had been immersed for a day (Figure S4). This signal indicated that the terephthalate ligand in the UiO-66 had been displaced by adipate. 2) Even after activation of the sample using supercritical (Sc) CO_2, which would remove all guest molecules and even weakly bound solvent molecules at the metal ions,[20] the resulting UiO-66-AD6-Sc still contained 22.4% adipic acid, as estimated from the ^{1}H NMR spectrum of a sample digested in [D_6]DMSO containing HF (Table S2). This result revealed that the adipate in the structure was strongly bound. Therefore, the most likely mode is 1:2 substitution for all of the UiO-66-AD*n*s, although 1:1 substitution may be mixed with 1:2 substitution in the case of UiO-66-AD6.

The PXRD patterns (Figure 3) of UiO-66-AD*n*s ($n=4$, 6, 8, and 10), obtained after activation by heat treatment at 100 °C, indicated that the structural regularities were retained even after ligand exchange and activation, although UiO-66-AD10 showed severe peak broadening. TEM images of the samples after removal of the guests indicated that the size and shape of UiO-66 were still maintained in the UiO-66-AD*n*s ($n=4$, 6, 8, and 10) (Figure S5). Thermogravimetric analysis data indicated that the desolvated UiO-66, UiO-66-AD4, UiO-66-AD6, and UiO-66-AD8 samples decomposed at 510 °C, whereas UiO-66-AD10 decomposed at a much lower temperature of 427 °C (Figure S6).

Distribution of substituted adipic acid in post-synthetically modified UiO-66

Although there have been several reports on partial ligand exchange of MOFs by post-synthetic modification, the location of the exchanged ligand has never been specified.[7,8] In this study, we investigated this issue after preparing UiO-66-AD6-1d and UiO-66-AD6-14d according to the same procedure as for UiO-66-AD6, but with immersion times of 1 day and 14 days, respectively, in the solution of the alkanedioic acid. We then assessed the distribution of the adipic acid incorporated in the crystal, and the dependence of the degree of ligand substitution on the immersion time of the sample in the adipic acid solution. To this end, a fixed amount of HF in [D_6]DMSO was added to various amounts of UiO-66-AD6-1d or UiO-66-AD6-14d samples, and the ratios of adipic acid/terephthalic acid were determined from the ^{1}H NMR spectra (see the Experimental Section). We anticipated that when only a very small amount of HF was added, only the surface of the MOF crystal would be digested, but as the amount of HF was increased, the inner part of the crystal would also be digested.

In the experiment, the minimum amount of HF required for complete digestion of UiO-66-AD6-1d was calculated based on the number of moles of carboxylate groups in the sample, and this was employed in the digestion. The results indicated that one equivalent of HF per carboxyl group was sufficient for complete digestion of the sample within 30 min. This fixed amount of HF diluted with [D_6]DMSO was then added to 2×, 4×, and 8× excesses of UiO-66-AD6-1d, respectively, and the samples were digested for 30 min. After digestion, ^{1}H NMR spectra were measured (see the Experimental Section). The contents of adipic acid were found to be 48%, 41%, and 32% for the 1/8, 1/4, and 1/2 digested samples, respectively, for UiO-66-AD6-1d. A totally digested UiO-66-AD6-1d sample showed a 20% content of adipic acid (Figure S7). The same digestion method was applied to UiO-66-AD6-14d. The contents of adipic acid were found to be 48%, 35%, 30%, and 22% for the 1/8, 1/4, 1/2, and totally digested samples, respectively.

These results indicated that the less digested samples had increased percentages of adipic acid, clearly demonstrating that the exchanged ligands in the solid were concentrated near the surface of the crystal rather than being homogeneously distributed throughout its interior. The results also showed that the immersion time did not affect the distribution of the adipic acid incorporated into the crystal.

Gas sorption properties and thermodynamic analyses of UiO-66 and UiO-66-AD*n*s

It has previously been reported that UiO-66 has a moderate CO_2 uptake capacity of 1.8 mmol g^{-1} at 1 bar and 298 K,[21] and that this capacity may be enhanced by the introduction of functional groups such as amino, nitro, methoxy, or naphthyl,[9] or by post-synthetic modification of the framework metal ions.[21] For example, when an amine functional group was introduced, the CO_2 adsorption capacity reached 3.0 mmol g^{-1} at 1 bar and 298 K.[21] When framework Zr^{IV} ions were replaced by Ti^{IV} ions, the CO_2 uptake was enhanced to 2.2 mmol g^{-1} at 1 bar and 298 K.[9]

Gas sorption isotherms of the present UiO-66-AD*n* samples were measured for N_2, CO_2, and CH_4 (Table 1). From the N_2 adsorption data at 77 K, the BET (Langmuir) surface areas and pore volumes were calculated and they are summarized in Table 1 (see the Experimental Section). UiO-66 has a BET surface area (pore volume) of 1057 $m^2 g^{-1}$ (0.441 $cm^3 g^{-1}$) whereas UiO-66-AD4, UiO-66-AD6, UiO-66-AD8, and UiO-66-AD10 have reduced surface areas of 942 $m^2 g^{-1}$ (0.351 $cm^3 g^{-1}$), 1020 $m^2 g^{-1}$ (0.421 $cm^3 g^{-1}$), 901 $m^2 g^{-1}$ (0.342 $cm^3 g^{-1}$), and 213 $m^2 g^{-1}$ (0.100 $cm^3 g^{-1}$), respectively. Interestingly, the surface area and pore volume of UiO-66-AD10 were much lower than those of the other samples. This might have been because the high loading of sebacic acid (50%) partially blocked the pores.

In contrast to the decreased N_2 uptakes of all of the UiO-66-AD*n*s at 77 K, the CO_2 adsorption capacities of UiO-66-AD6 at 273, 298, and 323 K were found to be greater than those of UiO-66. In particular, the decreases in the CO_2 adsorption capacities of UiO-66-AD6 at elevated temperatures are less significant than those of UiO-66 (Figure 4). As a result, the ratios of the CO_2 uptake of UiO-66-AD6 compared to that of UiO-66 increase from 1.20 at 273 K, to 1.34 at 298 K, and finally to 1.58 at 323 K. To gain insight into this behavior, the desorption functions (*G*, *H*, *S*) were calculated from the gas sorption data (see the Experimental Section).[14] These functions give values in units of energy per weight of a sample, and the data are presented in Figure 5. Since the values of Gibbs free energy, enthalpy, and entropy for gas adsorption in MOFs are generally negative, these functions are denoted as "desorption" functions. At 1 atm and 298 K, UiO-66-AD6 had the highest desorption free energy (8.29 kJ kg^{-1}), followed by UiO-66-AD4 (6.55 kJ kg^{-1}), UiO-66 (6.38 kJ kg^{-1}), and UiO-66-AD8 (6.30 kJ kg^{-1}). UiO-66-AD10 had the lowest CO_2 uptake and a fairly small desorption free energy (1.84 kJ kg^{-1}). In terms of desorption enthalpies and entropies, UiO-66-AD4 (69.4 kJ kg^{-1}, 211 J kg^{-1} K^{-1}), UiO-66-AD6 (65.3 kJ kg^{-1}, 191 J kg^{-1} K^{-1}), and UiO-66-AD8 (64.6 kJ kg^{-1}, 195 J kg^{-1} K^{-1}) showed around 20% higher values than UiO-66 (56.4 kJ kg^{-1}, 168 J kg^{-1} K^{-1}), whereas UiO-66-AD10 (25.3 kJ kg^{-1}, 78.8 J kg^{-1} K^{-1}) showed lower values than UiO-66 (Figure S8). For this series of compounds, the entropy values had a linear relationship with the enthalpy values (Figure 5). During the adsorption process, strong interactions between the gas molecules and the modified framework result in an increased entropy loss, counteracting the benefit of the enhanced enthalpy. However, UiO-66-AD6 deviated from this trend, leading to the highest desorption free energy among the compounds. In contrast to this irregular behavior of UiO-66-AD6 for CO_2 adsorption, no such deviation was seen for CH_4 adsorption in UiO-66 and the respective UiO-66-AD*n*s (Figure S9). The increased CO_2 uptake in UiO-66-AD6 must be attributed to relatively strong interactions between the CO_2 molecules and the carboxyl pendants of appropriate length. We assume that the length of the dangling adipic acid groups (5.796 Å; distance between the two carboxylate carbon atoms) is optimal to allow for multiple interaction modes with the CO_2 molecules in the pores, which increases the enthalpy loss and mitigates the entropy loss on CO_2 adsorption. The diagonal distance of an octahedral cage of UiO-66 is 15.737 Å, which is too long for two succinic acid ligands (3.594 Å × 2) and too short for two suberic acid ligands (7.885 Å × 2).

The isosteric heats (Q_{st}) of CO_2 and CH_4 adsorption were calculated by using the Clausius–Clapeyron (C–C) equation as well as the virial equation (Table 2 and Figures S10–S14).[1] When the virial equation was used, the Q_{st} values at zero coverage could be calculated. When the Q_{st} values were calculated with the C–C equation, the gas adsorption isotherms could be fitted to the Langmuir–Freundlich equation. In this case, the Q_{st} values diverged at zero coverage, and therefore the values at low coverage rather than zero coverage are given in Table 2. Depending on the amount of gas loading, the Q_{st} values obtained from the virial equation

Table 1. Gas adsorption data of UiO-66 and UiO-66-AD*n*s.

	T [K]	*P* [atm]	UiO-66 [mmol g^{-1}]	UiO-66-AD4 [mmol g^{-1}]	UiO-66-AD6 [mmol g^{-1}]	UiO-66-AD8 [mmol g^{-1}]	UiO-66-AD10 [mmol g^{-1}]
N_2	77	0.9	339[a]	247[a]	301[a]	241[a]	75[a]
CO_2	273	1.0	3.14	3.56	3.76	3.31	1.33
	298	1.0	1.96	1.92	2.63	1.83	0.57
	323	1.0	1.07	1.06	1.69	0.97	0.29
CH_4	273	1.0	0.84	0.84	0.89	0.85	0.17
	298	1.0	0.50	0.45	0.48	0.45	0.13
	323	1.0	0.20	0.19	0.27	0.14	0.10
Surface area [$m^2 g^{-1}$]			1057[b] (1098)[c]	942[b] (963)[c]	1020[b] (1038)[c]	901[b] (927)[c]	213[b] (224)[c]
Pore volume [$cm^3 g^{-1}$]			0.441	0.351	0.421	0.342	0.100

[a] In $cm^3 g^{-1}$. [b] BET surface area. [c] Langmuir surface area.

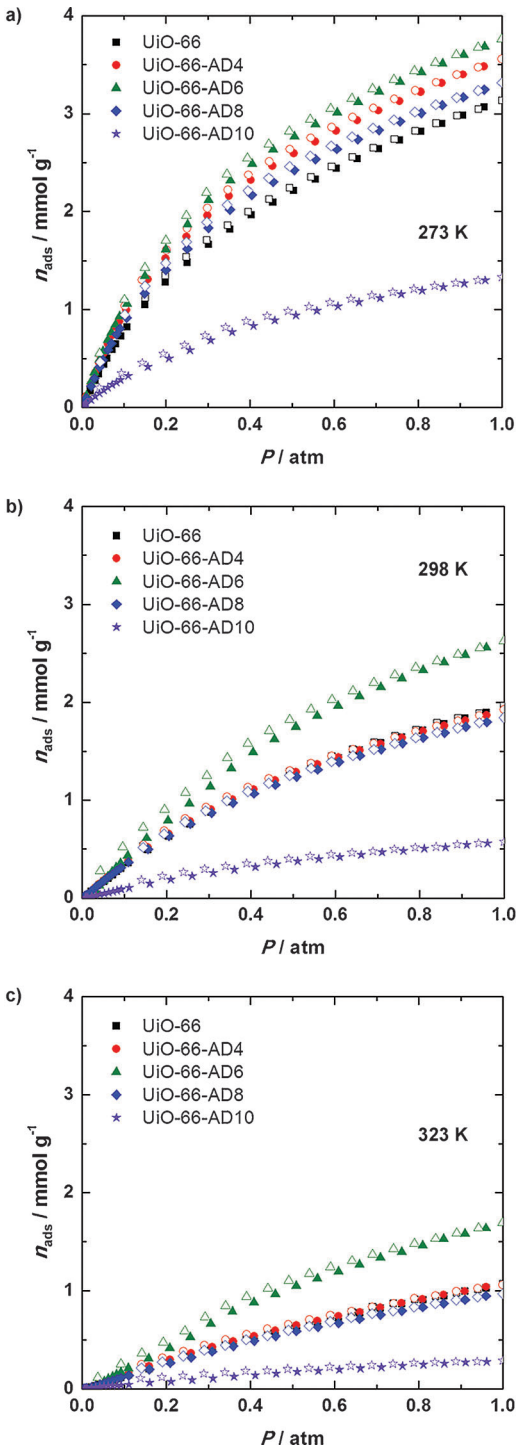

Figure 4. CO_2 adsorption isotherms at a) 273 K, b) 298 K, and c) 323 K for UiO-66 (■), UiO-66-AD4 (●), UiO-66-AD6 (▲), UiO-66-AD8 (◆), and UiO-66-AD10 (★). Filled shapes: adsorption; open shapes: desorption.

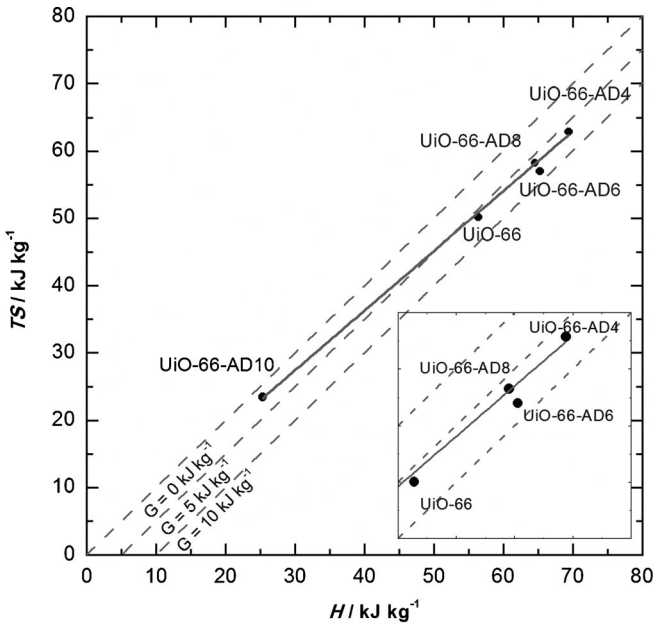

Figure 5. Linear relationship between the enthalpies and the entropies of CO_2 adsorption in UiO-66 and UiO-66-AD*n*s. Iso-value lines of the desorption free energy are drawn as dashed lines. The inset shows that the position of UiO-66-AD6 deviates from the regression line (solid line) by having reduced entropy, resulting in the highest desorption free energy value (8.29 kJ kg^{-1}), increased by 27% compared to that of UiO-66 (6.38 kJ kg^{-1}).

Table 2. Q_{st} values of various samples.

	Q_{st} of CO_2 [kJ mol^{-1}]		Q_{st} of CH_4 [kJ mol^{-1}]	
	Virial[a]	Clausius–Clapeyron[b]	Virial[a]	Clausius–Clapeyron[c]
UiO-66	40.73	34.96	37.17	29.16
UiO-66-AD4	45.72	35.27	34.36	30.43
UiO-66-AD6	49.85	36.65	37.51	31.60
UiO-66-AD8	44.56	35.90	24.69	25.83
UiO-66-AD10	50.77	34.19	19.94	23.58

[a] $n_{ads}=0$ mmol g^{-1}. [b] $n_{ads}=0.05$ mmol g^{-1}. [c] $n_{ads}=0.01$ mmol g^{-1}.

fluctuate around the Q_{st} values obtained from the C–C equation, since the virial equation contains polynomial terms. Regardless of the calculation method, the Q_{st} values for CO_2 adsorption increased for all of the UiO-66-AD*n*s compared with those for UiO-66, except for the Q_{st} value of UiO-66-AD10 calculated with the C–C equation. UiO-66-AD6 exhibited the highest Q_{st} values among all of the samples. In contrast to the CO_2 adsorption, the Q_{st} values for CH_4 adsorption were not simply increased by the carboxyl pendants. The Q_{st} values for CH_4 adsorption increased in UiO-66-AD6 and decreased in UiO-66-AD8 and UiO-66-AD10, regardless of the calculation method.

Selectivity estimated by ideal adsorption solution theory (IAST)

A selectivity coefficient of ideal adsorption solution is calculated by assuming that the free energies (G) of each gas adsorbed in a framework are identical at a fixed temperature (see the Experimental Section). The desorption free energy (G) is the same as πA, which is a product of spreading pressure and specific surface area used for describing the thermodynamics of surface adsorption.[14]

The selectivities for CO_2 adsorption over that of CH_4 at 273 K, 298 K, and 323 K were calculated to determine the ap-

Table 3. The CO_2/CH_4 separation parameters of UiO-66 and UiO-66-AD*n*s for landfill gas in the VSA process. The composition of landfill gas was assumed to be 50% CO_2 and 50% CH_4.

	T [K]	n_{CO_2} [mmol g^{-1}]	Δn_{CO_2} [mmol g^{-1}]	R[a]	α[b]
UiO-66	273	2.104	1.671	0.794	10.4
	298	1.184	1.017	0.859	6.87
	323	0.568	0.508	0.894	6.87
UiO-66-AD4	273	2.486	1.948	0.784	12.6
	298	1.211	1.031	0.851	8.04
	323	0.620	0.545	0.879	9.05
UiO-66-AD6	273	2.636	2.063	0.783	15.0
	298	1.598	1.415	0.885	10.0
	323	0.945	0.864	0.914	10.1
UiO-66-AD8	273	2.331	1.848	0.793	12.3
	298	1.170	0.998	0.853	7.31
	323	0.536	0.476	0.888	10.9
UiO-66-AD10	273	0.903	0.738	0.817	16.1
	298	0.342	0.295	0.863	9.29
	323	0.162	0.140	0.864	8.25

[a] R = regenerability. [b] α = IAST selectivity, calculated under desorption conditions (P = 0.1 atm).

plicability of UiO-66-AD*n*s for the separation of landfill gas by using the vacuum swing adsorption (VSA) process (Table 3 and Figure S15). The pressure of adsorption was taken as 1.0 atm and that of desorption as 0.1 atm in VSA.[22] The selectivity values were calculated under the desorption conditions (0.1 atm), because the adsorption data should be extrapolated to $P > 1$ atm to calculate the free energies of the CH_4 sorption under the adsorption conditions. For instance, single-component CH_4 gas adsorption data up to 4.0 atm at 298 K was required to calculate the IAST selectivity for the 1:1 mixture of CO_2 and CH_4 gases adsorbed on UiO-66 at 1 atm 298 K. The selectivity values for CO_2/CH_4 adsorption at 273 K calculated under the adsorption conditions did not converge in the case of UiO-66-AD10.

Four adsorbent evaluation criteria suggested by Snurr's group,[22] namely CO_2 uptake under adsorption conditions, working CO_2 capacity, regenerability (R), and selectivity (α), were also calculated and the data are presented in Table 3. For landfill gas separation, all of the UiO-66-AD*n*s showed significantly increased selectivity values for CO_2 adsorption over that of CH_4 compared to those of UiO-66. In particular, UiO-66-AD6 showed the highest selectivity values as well as the highest CO_2 uptake and the best working CO_2 capacity. Notably, the enhancement factors of the CO_2 uptake and the working CO_2 capacity in UiO-66-AD6 compared to those of UiO-66 increased with increasing temperature, from about 20% at 273 K to about 70% at 323 K.

Conclusion

We have prepared various UiO-66 derivatives, designated as UiO-66-AD*n*s, in which a series of flexible carboxylic acid pendants of various lengths has been incorporated by post-synthetic ligand exchange. We then proceeded to investigate the thermodynamic aspects of CO_2 adsorption in these systems. An unprecedented 1:2 ligand substitution of terephthalate in UiO-66 by two alkanedioate ligands has been identified. In particular, UiO-66-AD6, containing adipic acid pendants, has been found to exhibit a significantly enhanced CO_2 separation ability for landfill gas, showing enhanced working capacity and significantly increased selectivity for CO_2 adsorption over that of CH_4, compared to those of UiO-66 and the other UiO-66-AD*n*s. From an analysis of enthalpy and entropy, it was revealed that the increased CO_2 capacity of UiO-66-AD6 can be attributed to an increased enthalpy loss and a mitigated entropy loss upon CO_2 adsorption as a result of interaction with the dangling carboxyl pendants of appropriate length. These flexible carboxylic acid pendants effectively accommodate CO_2, reducing the entropy loss upon CO_2 adsorption. No such phenomenon is manifested in CH_4 adsorption due to weak interaction between the CH_4 molecules and the pendants. The present work has demonstrated that the introduction of dangling carboxyl pendants of appropriate length in an MOF by post-synthetic ligand exchange can enhance the CO_2 separation performance of the MOF at high temperatures.

Experimental Section

General methods

All chemicals and solvents used in the synthesis were of reagent grade and were used without further purification. Infrared spectra were recorded with a Perkin-Elmer Spectrum One FTIR spectrophotometer. NMR spectra were measured on a Bruker Advance DPX-300 spectrometer. Thermogravimetric analyses (TGA) were performed under N_2 (g) at a scan rate of 5 °C min^{-1}, using a TGA Q50 from TA Instruments. Powder X-ray diffraction data were recorded on a Bruker D8 Advance diffractometer operating at 40 kV and 40 mA and employing $Cu_{K\alpha}$ radiation (λ = 1.54050 Å), with a scan speed of 0.3 s per step and a step size of 0.02° in 2θ. TEM images were acquired with a Hitachi H-7600 operating at 100 kV.

Preparation of activated UiO-66

UiO-66 was prepared according to the previously reported method.[6] The as-synthesized UiO-66 was then sonicated in DMF/MeOH (1:1), collected by filtration, and washed successively with DMF (3×30 mL) and MeOH (3×30 mL). The sample was activated by heating at 100 °C under vacuum. UiO-66 immediately adsorbed 16 equivalents of H_2O molecules on exposure to air. FTIR (Nujol mull): $\tilde{\nu}$ = 3669, 3639, 3418 (OH^-), 1578 cm^{-1} (CO_2^-).

Preparation of UiO-66-AD*n* (*n* = 4, 6, 8, and 10) by ligand exchange of UiO-66 with alkanedioic acids followed by activation

Ligand-exchange experiments were performed according to the previously reported method.[8] Each alkanedioic acid (HO_2C-$(CH_2)_{n-2}CO_2H$, n = 4, 6, 8, and 10; 0.2 mmol) was dissolved in 4% aqueous KOH solution (2 mL). The solution was neutralized to pH 7 with 1 M HCl (total 3 mL). UiO-66 (ca. 57 mg, 0.2 mmol of terephthalate linkers) was immersed in the solution, which had been kept in a pre-heated oven (60 °C) for 1 h, and the mixture was allowed to stand for 5 days. After immersion, the mixture was centrifuged and the aqueous phase was decanted off. The solid was immersed in MeOH (10 mL), and the supernatant was exchanged with fresh

MeOH (10 mL) every 12 h for 2 days. The solid was collected by filtration and dried under vacuum at 100 °C for 12 h to afford the respective UiO-66-AD*n*. After gas sorption measurements, IR spectra of the samples were measured. Each UiO-66-AD*n* immediately adsorbed water molecules on exposure to air. For UiO-66-AD4, FTIR (Nujol mull): $\tilde{\nu}$ = 3669, 3638, 3390 (OH^-), 1703 (C=O), 1578 cm^{-1} (CO_2^-). For UiO-66-AD6, FTIR (Nujol mull): $\tilde{\nu}$ = 3669, 3639, 3411 (OH^-), 1718 (C=O), 1579 cm^{-1} (CO_2^-). For UiO-66-AD8, FTIR (Nujol mull): $\tilde{\nu}$ = 3670, 3640, 3418 (OH^-), 1709 (C=O), 1578 cm^{-1} (CO_2^-). For UiO-66-AD10, FTIR (Nujol mull): $\tilde{\nu}$ = 3672, 3641, 3383 (OH^-), 1703 (C=O), 1578 cm^{-1} (CO_2^-).

^{1}H NMR analysis of UiO-66-AD*n* (*n* = 4, 6, 8, and 10)

Each activated UiO-66-AD*n* (3 mg) was placed in a test tube and digested in [D_6]DMSO (580 μL) containing an aqueous solution of 4.8 wt% HF (20 μL). For accurate integration of NMR spectra, the water peak was suppressed.

Preparation of UiO-66-AD6-Sc by a supercritical CO_2 drying method

Prior to activation, a sample of UiO-66 that had been ligand exchanged with adipic acid for 5 days was exchanged with fresh MeOH for 2 days as described previously. The crystals were placed inside a supercritical dryer together with the solvent, and the drying chamber was sealed. The temperature was set at 45 °C and the pressure of the chamber was raised to 200 bar with CO_2. The chamber was vented at a rate of 10 mL min^{-1} and then refilled with CO_2. Cycles of refilling with CO_2, pressurizing, and venting were repeated for 5 h. After drying, the closed vessel containing the dried sample was transferred to a glove bag filled with argon to prevent exposure of the crystals to air. UiO-66-AD6-Sc immediately adsorbed 13 equivalents of H_2O molecules on exposure to air. FTIR (KBr pellet): $\tilde{\nu}$ = 3399 (OH^-), 2939 (C-H), 1574 cm^{-1} (CO_2^-).

Partial digestion of UiO-66-AD6–1d and UiO-66-AD6–14d

An aqueous solution of 4.8 wt% HF (11 μL, 0.026 mmol) was diluted with [D_6]DMSO (590 μL). UiO-66-AD6 (7 mg, 14 mg, or 28 mg, respectively), which had been dried at 100 °C overnight, was then immersed in the solution for 30 min. The molar ratio of HF to the number of carboxylate groups in UiO-66-AD6 was adjusted to 1:2, 1:4, and 1:8 in three digestion runs, respectively. For accurate integration of NMR spectra, the water peak was suppressed.

Low-pressure gas sorption measurements

Gas adsorption–desorption data were measured by means of an automated micropore gas analyzer (Autosorb-1 or Autosorb-3B; Quantachrome Instruments). All gases used were of 99.9999% purity. Samples were activated at 100 °C under vacuum for 12 h. The N_2 gas isotherms were measured at 77 K. The CO_2 and CH_4 gas isotherms were measured at 273 K, 298 K, and 323 K at each equilibrium pressure by the static volumetric method. After gas sorption measurement, the weight of the sample was precisely measured once more. Surface area was calculated from the N_2 adsorption data measured at 77 K using the Brunauer–Emmett–Teller (BET) and Langmuir methods by plotting the data points until the value of $n_{ads}(1-P/P^\circ)$ reached the maximum. Pore volume was calculated by applying the NLDFT (non-local density functional theory) equilibrium model to N_2 adsorption data measured at 77 K.

Calculation of thermodynamic functions (*G*, *H*, *S*) from gas adsorption isotherms

The desorption free energy (*G*) is the minimum work required for the isothermal release of adsorbed gas at a given temperature and pressure.[14] Under low pressure, the free energy of desorption can be calculated by Equation (1):

$$G = RT\int_0^P \frac{n}{P}\mathrm{d}P = RT\int_0^P n\mathrm{d}\ln P \tag{1}$$

For an adsorption isotherm fitted with Langmuir, dual-site Langmuir, and Langmuir–Freundlich equations, the free energy function (*G*) can be expressed in analytical form [Eq. (2)]. In this work, we applied the Langmuir–Freundlich equation to fit the adsorption isotherms for CO_2 and CH_4, and the desorption free energy function was obtained as Equation (3):

$$n = n_{\mathrm{m}}\frac{bP^{(1/t)}}{1+bP^{(1/t)}} \tag{2}$$

$$G = n_{\mathrm{m}}tRT\ln(1+bP^{(1/t)}) \tag{3}$$

The enthalpy of desorption (*H*) was calculated by applying the Gibbs–Helmholtz equation to the data obtained at multiple temperatures [Eq. (4)]:

$$H = -T^2\left[\frac{\partial(G/T)}{\partial T}\right]_P = \left[\frac{\partial(G/T)}{\partial(1/T)}\right]_P \tag{4}$$

The entropy of desorption was obtained as follows [Eq. (5)]:

$$S = -\left[\frac{\partial G}{\partial T}\right]_P = \frac{H-G}{T} \tag{5}$$

Calculation of IAST selectivity

The desorption free energies of adsorbed species are all the same under the equilibrium conditions at a fixed temperature. Therefore, selectivity (α) can be calculated by the following equations [Eqs. (6) and (7)]. For a given *G* value:

$$Py_i = P_i^\circ(G)x_i \tag{6}$$

$$\alpha_{i,j} = \frac{x_i/y_i}{x_j/y_j} = \frac{P_j^\circ(G)}{P_i^\circ(G)} \tag{7}$$

In this study, $P^\circ(G)$ was derived from Equation (3) [Eq. (8)]:

$$P^\circ(G) = \left(\left(\exp\left(\frac{G}{n_m tRT}\right)-1\right)/b\right)^t \tag{8}$$

The total pressure (*P*) and the total loading (*n*) are given by the following expressions [Eqs. (9) and (10)]:

$$P = \frac{1}{y_i/P_i^\circ + y_j/P_j^\circ} \tag{9}$$

$$\frac{1}{n} = \sum_i \frac{x_i}{n_i} \quad (10)$$

The individual loadings (n_i) are given as follows [Eq. (11)]:

$$n_i = nx_i \quad (11)$$

Abbreviations

α: Selectivity; b: Constant in Equation (2); n: amount adsorbed (mmol g^{-1}); n_m: Constant in Equation (2) (mmol g^{-1}); G: Gibbs free energy of desorption (kJ kg^{-1}); H: enthalpy of desorption (kJ kg^{-1}); P: Pressure (atm); P_i^o: pressure of pure component adsorption (atm): R: gas constant, 8.3145 J mol^{-1} K^{-1}; S: entropy of desorption (kJ kg^{-1} K^{-1}); t: constant in Equation (2); T: temperature (K); x_i: mole fraction of component i in adsorbed phase; y_i: mole fraction of component i in vapor phase.

Acknowledgements

This work was supported by a National Research Foundation (NRF) grant funded by the Korean Government (MSIP) (NRF-2012-055324 and NRF-2005-0049412). D.H.H. acknowledges support by Global Ph.D. Fellowship (GPF) programs of the NRF. We thank Sung-Soo Kim for obtaining the TEM images.

Keywords: carbon dioxide separation · carboxyl pendants · ligand substitution · metal–organic frameworks · post-synthetic modification · thermodynamics

[1] K. Sumida, D. L. Rogow, J. A. Mason, T. M. McDonald, E. D. Bloch, Z. R. Herm, T.-H. Bae, J. R. Long, *Chem. Rev.* **2012**, *112*, 724 – 781.
[2] S. Xiang, Y. He, Z. Zhang, H. Wu, W. Zhou, R. Krishna, B. Chen, *Nat. Commun.* **2012**, *3*, 954.
[3] J. J. Low, A. I. Benin, P. Jakubczak, J. F. Abrahamian, S. A. Faheem, R. R. Willis, *J. Am. Chem. Soc.* **2009**, *131*, 15834 – 15842.
[4] K. S. Park, Z. Ni, A. P. Côté, J. Y. Choi, R. Huang, F. J. Uribe-Romo, H. K. Chae, M. O'Keeffe, O. M. Yaghi, *Proc. Natl. Acad. Sci. USA* **2006**, *103*, 10186 – 10191.
[5] G. Férey, C. Mellot-Draznieks, C. Serre, F. Millange, J. Dutour, S. Surblé, I. Margiolaki, *Science* **2005**, *309*, 2040 – 2042.
[6] J. H. Cavka, S. Jakobsen, U. Olsbye, N. Guillou, C. Lamberti, S. Bordiga, K. P. Lillerud, *J. Am. Chem. Soc.* **2008**, *130*, 13850 – 13851.
[7] M. Kim, J. F. Cahill, H. Fei, K. A. Prather, S. M. Cohen, *J. Am. Chem. Soc.* **2012**, *134*, 18082 – 18088.
[8] M. Kim, J. F. Cahill, Y. Su, K. A. Prather, S. M. Cohen, *Chem. Sci.* **2012**, *3*, 126.
[9] C. H. Lau, R. Babarao, M. R. Hill, *Chem. Commun.* **2013**, *49*, 3634 – 3636.
[10] T. M. McDonald, W. R. Lee, J. A. Mason, B. M. Wiers, C. S. Hong, J. R. Long, *J. Am. Chem. Soc.* **2012**, *134*, 7056 – 7065.
[11] H. J. Park, Y. E. Cheon, M. P. Suh, *Chem. Eur. J.* **2010**, *16*, 11662 – 11669.
[12] T. Li, M. T. Kozlowski, E. A. Doud, M. N. Blakely, N. L. Rosi, *J. Am. Chem. Soc.* **2013**, *135*, 11688 – 11691.
[13] T. K. Prasad, D. H. Hong, M. P. Suh, *Chem. Eur. J.* **2010**, *16*, 14043 – 14050.
[14] A. Myers, *Adsorption* **2003**, *9*, 9 – 16.
[15] J. Seo, R. Matsuda, H. Sakamoto, C. Bonneau, S. Kitagawa, *J. Am. Chem. Soc.* **2009**, *131*, 12792 – 12800.
[16] N. Planas, A. L. Dzubak, R. Poloni, L.-C. Lin, A. McManus, T. M. McDonald, J. B. Neaton, J. R. Long, B. Smit, L. Gagliardi, *J. Am. Chem. Soc.* **2013**, *135*, 7402 – 7405.
[17] S. Henke, R. A. Fischer, *J. Am. Chem. Soc.* **2011**, *133*, 2064 – 2067.
[18] J. F. M. Denayer, R. A. Ocakoglu, I. C. Arik, C. E. A. Kirschhock, J. A. Martens, G. V. Baron, *Angew. Chem.* **2005**, *117*, 404 – 407; *Angew. Chem. Int. Ed.* **2005**, *44*, 400 – 403.
[19] Q. Yang, A. D. Wiersum, P. L. Llewellyn, V. Guillerm, C. Serre, G. Maurin, *Chem. Commun.* **2011**, *47*, 9603 – 9605.
[20] T. K. Kim, M. P. Suh, *Chem. Commun.* **2011**, *47*, 4258 – 4260.
[21] G. E. Cmarik, M. Kim, S. M. Cohen, K. S. Walton, *Langmuir* **2012**, *28*, 15606 – 15613.
[22] Y.-S. Bae, R. Q. Snurr, *Angew. Chem.* **2011**, *123*, 11790 – 11801; *Angew. Chem. Int. Ed.* **2011**, *50*, 11586 – 11596.

Received: September 28, 2013
Published online on December 20, 2013